DOI: 10.1002/anie.200503705

Isolation and Characterization of $Sc_2C_2@C_{68}$: A Metal-Carbide Endofullerene with a Non-IPR Carbon Cage[**]

Zhi-Qiang Shi, Xin Wu, Chun-Ru Wang, Xin Lu,* and Hisanori Shinohara**

The geometries of pure-carbon fullerenes synthesized thus far follow exclusively the isolated-pentagon rule (IPR), which states that the pentagons in the most stable fullerenes are isolated from each other by hexagons.[1,2] Due to enhanced steric strain (steric effect) and resonance destabilization pertaining to the pentalene-type 8π-electron system (electronic effect), pure-carbon non-IPR fullerenes with abutted pentagons are always unstable and synthetically unattainable.[3] However, it appears that non-IPR fullerenes can be stabilized by either endohedral inclusion of electron-donating metal atoms/clusters[4,5] or exohedral derivatization,[6] as exemplified by such non-IPR fullerene derivatives as the endofullerenes $Sc_2@C_{66}$,[4b] $La_2@C_{72}$,[4c] and $Sc_3N@C_{68}$[5] as well as the exohedral derivative $C_{50}Cl_{10}$.[6] On the other hand, many metal-carbide endofullerenes, for example, $Sc_2C_2@C_{84}$,[7] $Ti_2C_2@C_{78}$,[8] $Y_2C_2@C_{82}$,[9] and $Sc_3C_2@C_{80}$,[10] have been synthesized and characterized exclusively with IPR-satisfying fullerene cages. Herein we report the isolation and characterization of $Sc_2C_2@C_{68}$, which is, to the best of our knowledge, the first metal-carbide endofullerene having a non-IPR cage.

---

[*] Dr. Z.-Q. Shi, Prof. Dr. C.-R. Wang
Institute of Chemistry
Chinese Academy of Sciences
Beijing 100080 (China)
Fax: (+86) 10-6265-2120
E-mail: crwang@iccas.ac.cn

X. Wu, Prof. Dr. X. Lu
State Key Laboratory of Physical Chemistry of Solid Surface &
Center for Theoretical Chemistry
Departmental of Chemistry
Xiamen University
Xiamen 361005 (China)
Fax: (+86) 592-218-3047
E-mail: xinlu@xmu.edu.cn

Prof. Dr. H. Shinohara
Department of Chemistry
Nagoya University
Nagoya, 464-8602 (Japan)
Fax: (+81) 52-789-2962
E-mail: noris@cc.nagoya-u.ac.jp

[**] C.-R.W. thanks NSFC (No. 50225206, 90206045, 20121301), National Key Project on Basic Research (Grant 2006CB30040, 2003CB716900), and National Center for Nanoscience and Technology of China. X.L. thanks NSFC (No. 20021002, 20425312, 20203013, 20423002, 90206038). H.S. thanks the JSPS for Future Program on New Carbon Nano-Materials for Financial support.

Supporting information for this article is available on the WWW under http://www.angewandte.org or from the author.

The synthesis and isolation of Sc_2C_{70} are essentially analogous to those of other scandium metallofullerenes such as $Sc_2@C_{66}$ and $Sc_2C_2@C_{84}$ reported before.[4b,7] Briefly, soot containing Sc_2C_{70} and other metallofullerenes were generated by arc discharge of scandium/graphite carbide composite rods (Tokyo Tanso Co. Ltd., $12 \times 12 \times 300$ mm, 1.6 atom% Sc) in direct-current mode (350 A, 21 V) under a $17\,L\,min^{-1}$ flow of helium at 50–100 Torr. The soot was Soxhlet-extracted with carbon disulfide for 12 h, and the soot extracts were redissolved in toluene. Sc_2C_{70} was isolated by multistage HPLC with two complementary types of column (5PYE and Buckyclutcher columns). The retention time of Sc_2C_{70} on the 5PYE column is very close to that of C_{76}; thus, stage 1 was HPLC on the 5PYE column to roughly separate Sc_2C_{70} and C_{76} from C_{60}, C_{70}, and higher fullerenes and metallofullerenes. In stage 2, recycling HPLC on the 5PYE column was performed to separate Sc_2C_{70} from C_{76}. After 8–10 cycles, separation into two subfractions was completed, whereby the first subfraction (pink) was Sc_2C_{70} with some minor impurities and the second subfraction (yellow) was C_{76}. In stage 3, recycling HPLC on the Buckyclutcher column was performed to further purify the Sc_2C_{70}. The purity (up to 99%) of isolated Sc_2C_{70} was confirmed by laser-desorption time-of-flight (LD-TOF) mass spectrometry (Figure 1 a).

The relative yield of Sc_2C_{70} is roughly 0.1% of that of C_{70}. We isolated about 3 mg of Sc_2C_{70} (black powder) for spectroscopic study and structural characterization. Solutions of Sc_2C_{70} in carbon disulfide or toluene are pink. The UV/Vis/NIR spectrum of Sc_2C_{70} in carbon disulfide solution shows absorption peaks at 570, 841, and 1126 nm (Figure 1 b), and it differs remarkably from that of empty C_{70} (absorptions at 472, 550, and 640 nm). The remote absorption onset of Sc_2C_{70} at about 1800 nm (≈ 0.69 eV) as compared to that of C_{70} at about 680 nm identifies it as a metallofullerene with a small band gap.

The ^{13}C NMR spectrum of Sc_2C_{70} in CS_2 solution is shown in Figure 1 c. Between $\delta = 135$ and 158 ppm, the spectrum consists of a series of 21 distinct lines that indicate at least 21 unique C atoms in as-prepared Sc_2C_{70}. Except for an impurity peak at 137.5 ppm (Figure 1 c), a wider range spectrum (not shown) shows no further resonances attributable to impurities.

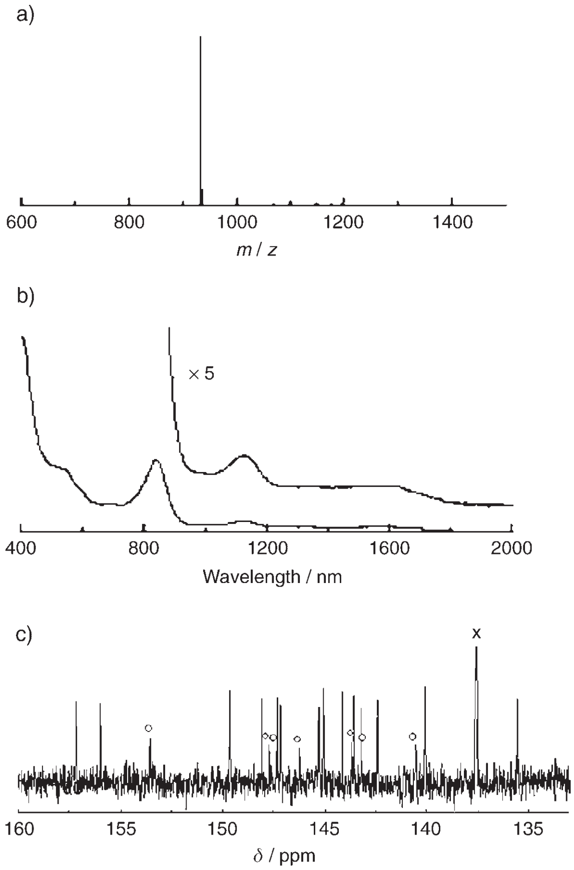

Figure 1. a) Time-of-flight mass spectrum of Sc_2C_{70} anions. b) UV/Vis/NIR absorption spectrum of Sc_2C_{70} in CS_2 solution. c) 125 MHz ^{13}C NMR spectrum of Sc_2C_{70} in CS_2 solution (27 °C, 100 000 scans (5 d) on a Varian Inova-600 spectrometer; chromium(III) acetylacetonate was added as relaxation agent). The 21 distinct ^{13}C NMR lines are located at 135.57 (7.4), 140.09 (8.5), 140.53 (3.3), 142.38 (7.3), 143.17 (3.7), 143.22 (7.0), 143.57 (7.7), 143.65 (4.1), 144.14 (8.0), 145.05 (8.3), 145.26 (6.7), 146.23 (3.0), 147.16 (6.8), 147.3 (7.5), 147.35 (3.1), 147.74 (3.2), 148.09 (7.4), 149.62 (8.1), 153.54 (3.8), 155.95 (7.0), and 157.18 ppm (7.1), where the data in parentheses refer to relative intensity. The line marked with × is assigned to impurities on account of its unusual line width and unreasonably high intensity.

With respect to the structure of Sc_2C_{70}, two models were considered: simple endohedral $Sc_2@C_{70}$ structure **1** and metal-carbide $Sc_2C_2@C_{68}$ structure **2**. For the simple endohedral $Sc_2@C_{70}$ structure, both the IPR-satisfying D_{5h}-symmetric C_{70} fullerene and all non-IPR C_{70} isomers that have 21 unique C atoms (i.e., #62, #3783, #4912, #6108, #7032, #7114, #8143 following the spiral algorithm[2]) were considered (Supporting Information). To attain a stable closed-shell electronic configuration,[8a,11,12] it is likely that a total of six valence electrons of the two encased Sc atoms would be donated to the carbon cage[13] to give a valence state of $(Sc^{3+})_2@C_{70}{}^{6-}$. Hence, we computed the structures of the hexaanions of the aforementioned C_{70} isomers at the semiempirical PM3[14] level of theory. In addition, the tetraanions and dianions of these C_{70} isomers were considered. The energies of the non-IPR $C_{70}{}^{q-}$ ($q = 2$, 4, 6) isomers are much higher than that of the IPR-satisfying D_{5h}-symmetric $C_{70}{}^{q-}$ ($q = 2$, 4, 6) predicted by the B3LYP[15]/6-31G//PM3 calculations[16] (Supporting Information). Hence, the $Sc_2@C_{70}$ structure **1** would preferentially adopt the IPR-satisfying D_{5h}-symmetric C_{70} cage, rather than any of the C_{2v}-symmetric non-IPR C_{70} cages. Though the D_{5h}-C_{70} cage has only five unique C atoms, encapsulation of Sc_2 in the D_{5h}-C_{70} cage can result in C_{2v}-symmetric geometries for $Sc_2@C_{70}$, which would give rise to 21 lines in the ^{13}C NMR spectrum. However, such a simple endohedral model is not supported by our quantum chemical calculations. The most stable C_{2v}-symmetric structure of $Sc_2@C_{70}$ (**1**) with D_{5h}-symmetic C_{70} cage, optimized at the GGA-PBE/DNP level of theory,[17,18] is shown in Figure 2; each Sc atom is bonded to a 5–6 ring fusion pertaining to the polar pentagon. The valence state of **1** is $(Sc^{2+})_2@(C_{70})^{4-}$; its HOMO consists predominantly of the d orbitals of the encased Sc^{2+} atoms (Supporting Information). Interestingly, a small barrier of only 1.6 $kcal\,mol^{-1}$ (at transition state **1_TS**) is predicted for rotation of the Sc_2 unit around the C_5 axis of C_{70} at room

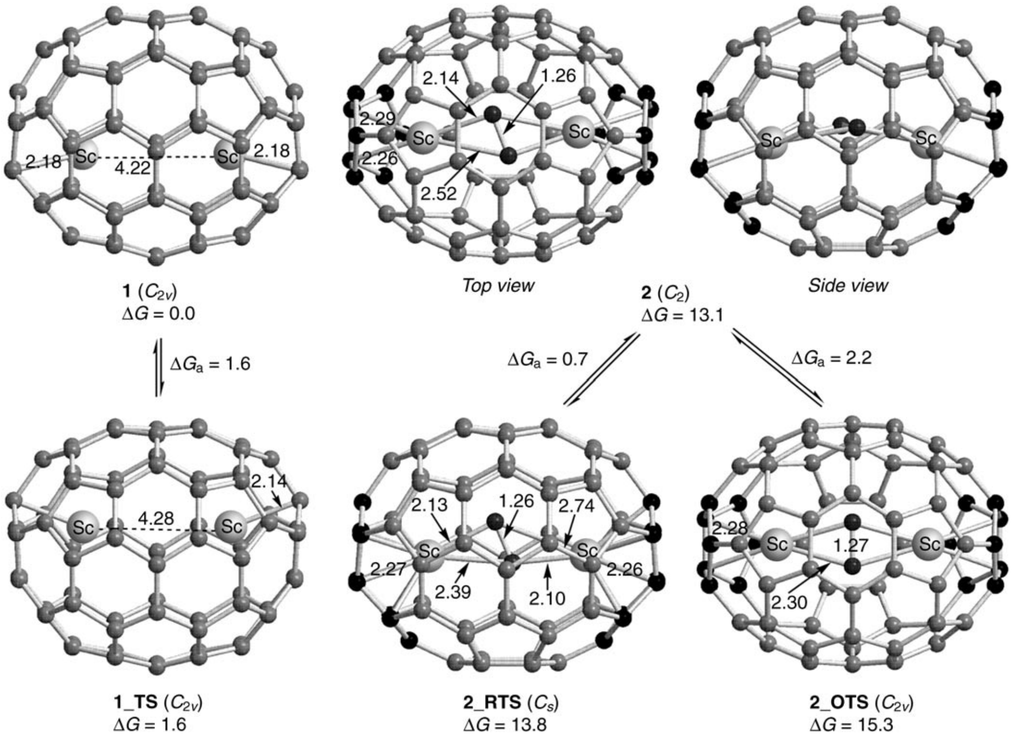

Figure 2. GGA-PBE/DNP predicted geometries (bond lengths [Å]), symmetries, and relative Gibbs free energies ΔG [kcal mol^{-1}] of Sc_2C_{70} isomers at $T = 298.15$ K. **1** is the optimized geometry of $Sc_2@C_{70}$; **1_TS** is the transition state for rotation of the Sc_2 unit around the C_5 axis of the D_{5h}-C_{70} cage. **2** is the optimized geometry of $Sc_2C_2@C_{68}$ with the non-IPR C_{68} (#6073) cage; **2_RTS** and **2_OTS** are the transition states for rotation and oscillation of the carbide moiety within **2**. These stationary points were confirmed to be local minima or transition states by harmonic vibrational analyses. ΔG_a [kcal mol^{-1}] is the free energy of activation for intramolecular rotation or oscillation.

temperature. Hence, rotation of the Sc_2 unit should be quite fast, and the C_{70} cage in **1** should maintain D_{5h} symmetry over a long timescale. As a result, $Sc_2@C_{70}$ (**1**) should display only five ^{13}C NMR lines at room temperature, in obvious disagreement with the measured spectrum shown in Figure 1 c. Hence, the synthesized Sc_2C_{70} does not exist in the $Sc_2@C_{70}$ form.

An alternative structural model for Sc_2C_{70} is $Sc_2C_2@C_{68}$ (**2**). According to the spiral algorithm,[2] C_{68} has no IPR-satisfying isomer but 6332 non-IPR isomers, of which only four C_{2v}-symmetric non-IPR isomers (i.e., #494, #465, #647, and #6073[2]) can produce 21 distinct lines in the ^{13}C NMR spectrum (Supporting Information). Among all 6332 non-IPR C_{68} isomers, C_{68} (#6073) has the smallest number (two) of pentagon–pentagon fusions. On the other hand, previous DFT computations on the metal-carbide endofullerene $Sc_2C_2@C_{84}$ revealed that the encased Sc_2C_2 cluster adopts the charge state $[Sc_2C_2]^{4+}$.[7b] Similarly, $Sc_2C_2@C_{68}$ (**2**) may have a charge state of $[Sc_2C_2]^{4+}@C_{68}{}^{4-}$ by donation of four electrons from the encased Sc_2C_2 cluster to the C_{68} cage. We computed structures and energies for the tetraanions of the four C_{2v}-symmetric non-IPR C_{68} isomers at the PM3 level of theory[14] and found that the $C_{68}{}^{4-}$(#6073) isomer is far more stable than the other three $C_{68}{}^{4-}$ isomers (Supporting Information). Hence $Sc_2C_2@C_{68}$ (**2**) would preferentially adopt the C_{2v}-symmetric C_{68} (#6073) cage. For Sc_2C_2 encased in the C_{68}(#6073) cage, the most stable structure **2** predicted at the GGA-PBE/DNP level is C_2-symmetric (Figure 2). Although the computed free energy of **2** is 13.1 kcal mol^{-1} higher than that of **1**, the much larger predicted HOMO–LUMO gap of **2** (0.68 eV) relative to **1** (0.33 eV) suggests that **2** is kinetically more stable than **1**. More importantly, **2** has a normal valence state $(Sc^{3+})_2(C_2)^{2-}@C_{68}{}^{4-}$ that fulfills the rule of closed-shell electronic configuration,[8a,11,12] whereas $Sc_2@C_{70}$ (**1**) has the valence state $(Sc^{2+})_2@(C_{70})^{4-}$, which contains unusual Sc^{2+} cations.[13,19] Hence, $Sc_2C_2@C_{68}$ (**2**) is chemically more rational than $Sc_2@C_{70}$ (**1**). As shown in Figure 3, the two highest occupied molecular orbitals (HOMO and HOMO$-$1) and two lowest unoccupied molecular orbitals (LUMO and LUMO$+$1) of **2** are derived mainly from the orbitals of the $C_{68}{}^{4-}$ cage with minor contribution from the encased cluster. These frontier orbitals should control the redox properties of **2**, for example, electrochemical redox potentials.

Furthermore, two transition states, **2_RTS** and **2_OTS**, were located for rotation of the encased acetylide ($C_2{}^{2-}$) group around the Sc–Sc axis and oscillation of the carbide moiety between the two Sc atoms, respectively (Figure 2). At room temperature, the rotational barrier (at **2_RTS**) is only 0.7 kcal mol^{-1}, whereas the barrier for the oscillation is 2.2 kcal mol^{-1} (at **2_OTS**). Due to the small barriers, rotation and oscillation of the encased carbide moiety within **2** should be rather fast at room temperature. Its C_{68} cage appears to be C_{2v}-symmetric by averaging over all rotating and oscillating structures on a long timescale, and this accounts for the observed 21 lines in the ^{13}C NMR spectrum. Accordingly, the synthesized Sc_2C_{70} can be reasonably assigned as $Sc_2C_2@C_{68}$ (**2**).

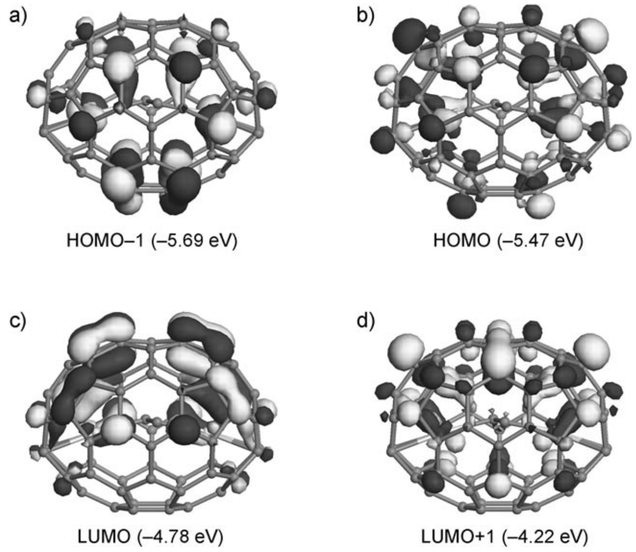

Figure 3. a, b) The two highest occupied molecular orbitals (HOMO and HOMO−1), and c, d) the two lowest unoccupied molecular orbitals (LUMO and LUMO+1) of $Sc_2C_2@C_{68}$ (**2**).

On account of the fascinating intramolecular dynamics of **2**, an accurate theoretical simulation of its ^{13}C NMR spectrum is nontrivial and requires molecular dynamics (MD) simulation followed by elaborate ^{13}C NMR computations on a large number of individual snapshots selected from the MD trajectory. Such a computational technique, though rather time-consuming, proved to be powerful in reproducing the experimental NMR spectrum of $Sc_3N@C_n$ ($n = 68$, 80).[20] Unfortunately, we cannot afford such a simulation due to hardware limitations. Nevertheless, we computed the ^{13}C NMR chemical shifts of **2** at the GIAO[21]-B3LYP/6-31G* level of theory using the B3LYP/6-31G* optimized geometries.[22] By averaging the chemical shifts of equivalent sites in the C_{68} cage, a total of 21 ^{13}C NMR chemical shifts ranging from 133.5 to 159.9 ppm were predicted for $Sc_2C_2@C_{68}$ (Supporting Information), in reasonable agreement with the experimental data, which range from 135.6 to 157.2 ppm. On the contrary, the computed ^{13}C NMR chemical shifts for static C_{2v}-symmetric $Sc_2@C_{70}$ (**1**) (Supporting Information) range from 130.1 to 159.4 ppm with an interval ($\Delta\delta = 29.3$ ppm) much larger than the experimental one ($\Delta\delta = 21.6$ ppm). So far as its intramolecular dynamic behavior is considered, **1** would display only five ^{13}C NMR signals ranging from 137.6 to 145.2 ppm (Supporting Information), inconsistent with the experimental spectrum (Figure 1c). These data further justify the $Sc_2C_2@C_{68}$ (**2**) structure for the synthesized Sc_2C_{70}. In addition, the predicted ^{13}C NMR chemical shift for the encapsulated acetylide group in $Sc_2C_2@C_{68}$ (**2**) is about 234.7 ppm, which is not observed in the NMR experiment, probably due to spin–rotation interaction[9] at room temperature.

Finally, it is noteworthy that the C_{68} cage of $Sc_2C_2@C_{68}$ (**2**) is different from that of the previously synthesized $Sc_3N@C_{68}$ (**3**).[5] Endofullerene **2** has the valence state $(Sc^{3+})_2(C_2)^{2-}@C_{68}{}^{4-}$, in which the C_{2v}-symmetric C_{68} (#6073) cage has two pentagon–pentagon pairs accommodating two Sc^{3+} ions. $Sc_3N@C_{68}$ (**3**) is in a valence state $(Sc^{3+})_3N^{3-}@C_{68}{}^{6-}$; its D_3-symmetric C_{68} (#6140) cage has three pentagon–pentagon pairs, each coordinated to an Sc^{3+} ion.[5,23] Accordingly, our synthesis of $Sc_2C_2@C_{68}$, in combination with the previous work on $Sc_3N@C_{68}$, clearly evidences that endohedral clusters such as Sc_2C_2 and Sc_3N function as templates for the synthesis of different non-IPR C_{68} cages.

Received: October 19, 2005
Revised: December 20, 2005

Keywords: density functional calculations · fullerenes · host–guest systems · scandium · structure elucidation

[1] H. W. Kroto, *Nature* **1987**, *329*, 529.
[2] P. W. Fowler, D. E. Manoloupoulos, *An Atlas of Fullerenes*, Oxford University Press, Oxford, **1995**.
[3] X. Lu, Z. Chen, *Chem. Rev.* **2005**, *105*, 3643.
[4] a) K. Kobayashi, S. Nagase, M. Yoshida, E. Osawa, *J. Am. Chem. Soc.* **1997**, *119*, 12693; b) C.-R. Wang, T. Kai, T. Tomiyama, T. Yoshida, Y. Kobayashi, E. Nishibori, M. Takata, M. Sakata, H. Shinohara, *Nature* **2000**, *408*, 426; c) H. Kato, A. Taninaka, T. Sugai, H. Shinohara, *J. Am. Chem. Soc.* **2003**, *125*, 7782.
[5] S. Stevenson, P. W. Fowler, T. Heine, J. C. Duchamp, G. Rice, T. Glass, K. Harich, E. Hajdu, R. Bible, H. C. Dorn, *Nature* **2000**, *408*, 428.
[6] a) S. Y. Xie, F. Gao, X. Lu, R. B. Huang, C.-R. Wang, X. Zhang, M. L. Liu, S. L. Deng, L. S. Zheng, *Science* **2004**, *304*, 699; b) X. Lu, Z. Chen, W. Thiel, P. v. R. Schleyer, R. B. Huang, L. S. Zheng, *J. Am. Chem. Soc.* **2004**, *126*, 14871; c) Z. Chen, *Angew. Chem.* **2004**, *116*, 4794; *Angew. Chem. Int. Ed.* **2004**, *43*, 4690.
[7] a) C.-R. Wang, T. Kai, T. Tomiyama, T. Yoshida, Y. Kobayashi, E. Nishibori, M. Takata, M. Sakata, H. Shinohara, *Angew. Chem.* **2001**, *113*, 411; *Angew. Chem. Int. Ed.* **2001**, *40*, 397; b) M. Krause, M. Hulman, H. Kuzmany, O. Dubay, G. Kresse, G. Seifert, C.-R. Wang, H. Shinohara, *Phys. Rev. Lett.* **2004**, *93*, 137403.
[8] a) K. Tan, X. Lu, *Chem. Commun.* **2005**, 4444; b) B. Cao, M. Hasegawa, K. Okada, T. Tomiyama, T. Okazaki, K. Suenaga, H. Shinohara, *J. Am. Chem. Soc.* **2001**, *123*, 9679; c) T. Yumura, Y. Sato, K. Suenaga, S. Iijima, *J. Phys. Chem. B* **2005**, *109*, 20251.
[9] a) T. Inone, T. Tomiyama, T. Sugai, H. Shinohara, *Chem. Phys. Lett.* **2003**, *382*, 226; b) T. Inone, T. Tomiyama, T. Sugai, T. Okazaki, T. Suematsu, N. Fujii, H. Utsumi, K. Nojima, H. Shinohara, *J. Phys. Chem. B* **2004**, *108*, 7573.
[10] Y. Iiduka, T. Wakahara, T. Nakahodo, T. Tsuchiya, A. Sakuraba, Y. Maeda, T. Akasaka, K. Yoza, E. Horn, T. Kato, M. T. H. Liu, N. Mizorogi, T. Kobayashi, S. Nagase, *J. Am. Chem. Soc.* **2005**, *127*, 12500.
[11] D. M. P. Mingos, T. Slee, Z. Lin, *Chem. Rev.* **1990**, *90*, 383, and references therein.
[12] a) H. W. Kroto, *Nature* **1987**, *329*, 529; b) P. W. Fowler, *J. Phys. Chem. Solids* **1993**, *54*, 1825; c) M.-F. Fan, Z. Lin, S. Yang, *J. Mol. Struct.* **1995**, *373*, 231; d) P. W. Fowler, F. Zerbetto, *Chem. Phys. Lett.* **1995**, *243*, 36.
[13] Sc^{2+} was long supposed in $Sc@C_{82}$ and $Sc_2@C_{84}$, but recent theoretical and experimental investigations revealed it is Sc^{3+} in either endofullerene: a) J. Lu, X. W. Zhang, X. G. Zhao, S. Nagase, K. Kobayashi, *Chem. Phys. Lett.* **2000**, *332*, 219; b) T. Pichler, Z. Hu, C. Grazioli, S. Legner, M. Knupfer, M. S. Golden, J. Fink, F. M. F. de Groot, M. R. C. Hunt, P. Rudolf, R. Follath, C. Jung, L. Kjeldgaard, P. Bruhwiler, M. Inakuma, H. Shinohara, *Phys. Rev. B* **2000**, *62*, 13196, and references therein.
[14] J. J. P. Stewart, *J. Comput. Chem.* **1989**, *10*, 209.

[15] For the hybrid density functional B3LYP method, see a) A. D. Becke, *J. Chem. Phys.* **1993**, *98*, 5648; b) C. Lee, W. Yang, R. G. Parr, *Phys. Rev. B* **1988**, *37*, 785.

[16] For each anion, the total energy was computed at the B3LYP/6-31G level with use of its PM3 optimized geometry. The calculations were performed with the Gaussian 98 suite of programs: Gaussian 98 (Revision A.7), M. J. Frisch, G. W. Trucks, H. B. Schlegel, G. E. Scuseria, M. A. Robb, J. R. Cheeseman, V. G. Zakrzewski, J. A. Montgomery, R. E. Stratmann, J. C. Burant, S. Dapprich, J. M. Millam, A. D. Daniels, K. N. Kudin, M. C. Strain, O. Farkas, J. Tomasi, V. Barone, M. Cossi, R. Cammi, B. Mennucci, C. Pomelli, C. Adamo, S. Clifford, J. Ochterski, G. A. Petersson, P. Y. Ayala, Q. Cui, K. Morokuma, D. K. Malick, A. D. Rabuck, K. Raghavachari, J. B. Foresman, J. Cioslowski, J. V. Ortiz, B. B. Stefanov, G. Liu, A. Liashenko, P. Piskorz, I. Komaromi, R. Gomperts, R. L. Martin, D. J. Fox, T. Keith, M. A. Al-Laham, C. Y. Peng, A. Nanayakkara, C. Gonzalez, M. Challacombe, P. M. W. Gill, B. G. Johnson, W. Chen, M. W. Wong, J. L. Andres, M. Head-Gordon, E. S. Replogle, J. A. Pople, Gaussian, Inc., Pittsburgh, PA, **1998**..

[17] For GGA-PBE density functional theory, see J. P. Perdew, K. Burke, M. Ernzerhof, *Phys. Rev. Lett.* **1996**, *77*, 3865.

[18] DNP refers to double numerical basis sets plus polarization. The GGA-PBE/DNP calculations were performed with the Dmol^3 code implemented in Material Studio, Accelrys Inc.: a) B. Delley, *J. Chem. Phys.* **1990**, *92*, 508; b) B. Delley, *J. Chem. Phys.* **2000**, *113*, 7756.

[19] F. A. Cotton, G. C. Wilkinson, A. Murillo, M. Bochmann, *Advanced Inorganic Chemistry*, 6th ed., Wiley-Interscience, New York, **1999**, p. 221.

[20] a) J. U. Reveles, T. Heine, A. M. Köster, *J. Phys. Chem. A* **2005**, *109*, 7068; b) T. Heine, K. Vietze, G. Seifert, *Magn. Reson. Chem.* **2004**, *42*, 199; c) "Fullerenes": T. Heine in *Calculation of NMR and EPR Parameters: Theory and Applications* (Eds.: M. Kaupp, V. G. Malkin, M. Bühl), Wiley-VCH, Weinheim, **2004**.

[21] K. Wolinski, J. F. Hilton, P. J. Pulay, *J. Am. Chem. Soc.* **1990**, *112*, 8251, and references therein.

[22] The GIAO-B3LYP/6-31G* theory proved to be sufficiently accurate in reproducing ^{13}C NMR chemical shifts of fullerenes (e.g., C_{60}, C_{70}, C_{76}, and C_{78}) and the endofullerene $Sc_3N@C_{80}$ (II): a) G. Sun, M. Kertesz, *J. Phys. Chem. A* **2000**, *104*, 7398; b) J. C. Duchamp, A. Demortier, K. R. Fletcher, D. Dorn, E. B. Iezzi, T. Glass, H. C. Dorn, *Chem. Phys. Lett.* **2003**, *375*, 655.

[23] J. M. Campanera, C. Bo, J. M. Poblet, *Angew. Chem.* **2005**, *117*, 7396; *Angew. Chem. Int. Ed.* **2005**, *44*, 7230.